Jpn. J. Pharmacol. **88**, 341 – 350 (2002)

Electrophysiological, Anatomical and Histological Remodeling of the Heart to AV Block Enhances Susceptibility to Arrhythmogenic Effects of QT-Prolonging Drugs

Atsushi Sugiyama[1,*], Yuko Ishida[1], Yoshioki Satoh[1], Shigeki Aoki[2], Masaaki Hori[2], Yasuki Akie[1], Yoshihiko Kobayashi[3] and Keitaro Hashimoto[1]

[1]*Department of Pharmacology,* [2]*Department of Radiology and* [3]*Second Department of Pathology, Yamanashi Medical University, Tamaho-cho, Nakakoma-gun, Yamanashi 409-3898, Japan*

Received September 27, 2001 Accepted December 19, 2001

ABSTRACT—The present study was designed to investigate what kinds of adaptation occurred in the canine chronic AV block model, which has been used to study torsade de pointes (TdP). Dogs at 7 – 10 days (acute phase) and 28 – 56 days (chronic phase) after AV block were assessed. Ventricular effective refractory period and monophasic action potential duration were prolonged in chronic animals compared with acute animals; moreover the electrically vulnerable period was prolonged in chronic animals. Non-specific I_{Kr} channel blocker cisapride (1 and 10 mg/kg, p.o.) was administered without anesthesia to estimate the feasibility of QT prolongation. In chronic animals, QT prolongation followed by TdP was induced in one dog by the low dose and in all by the high dose, which was not observed in acute animals. MR images indicated increases of diameter and wall thickness of both ventricles in chronic animals. The degree of hypertrophy was prominent in the right ventricular wall and septal wall. Heart weight of the chronic animals was 1.7 times greater than that of normal control subjects. Photo- and electron-micrograph analyses showed myocardial cell hypertrophy with parallel increases of collagen fiber and extracellular space in chronic animals. These electrophysiological, anatomical and histological adaptations may predispose the chronic AV block heart to drug-induced QT prolongation with enhanced risk of re-entry and early afterdepolarization, leading to the onset of TdP.

Keywords: Long QT syndrome, AV block, Monophasic action potential, Holter ECG, MR image

Since drug-induced prolongation of the QT interval is often associated with the onset of torsade de pointes (TdP), the interest in animal models of TdP arrhythmias has considerably increased (1, 2). The dog with chronic AV block has been used as a very suitable large-animal model for the study of TdP, both under conscious (3) and anesthetized circumstances (4 – 10). Previous studies revealed that the functional adaptations predispose the canine AV block heart to acquired TdP (4, 6, 8 – 10). Namely, QT interval and ventricular endocardial monophasic action potential (MAP) duration are much longer than expected from the bradycardia alone largely because of the reduction of I_{Ks} and I_{Kr} (4 – 6). Moreover, early afterdepolarization and interventricular dispersion of repolarization have been suggested to play major roles in the genesis of acquired TdP (8 – 10). However, it is still difficult to correlate the premature depolarization (trigger) and the dispersion of repolarization (substrate) to the occurrence of TdP.

The present study was designed to investigate electrophysiological, anatomical and histological adaptation possibly related to the facilitated occurrence of TdP in the AV block heart. For this purpose, we first examined the local changes of the final repolarization phase of the action potential, since the spatial proarrhythmic substrates should locate in adjoining sites involved in the perpetuation of the arrhythmias (11). AV block was induced in dogs using a recently introduced catheter ablation technique for dogs (12), which is much less invasive compared with the previously described surgical method, but requires skillful catheter manipulation technique (3, 4). The difference of the final repolarization phase was compared between acute (7 – 10 days after the AV block induction) and chronic phase (28 – 56 days after the AV block induction) by measuring the ventricular MAP and effective refractory period (ERP) from the same site (12 – 17). Next, feasibility of QT

*Corresponding author. FAX: +81-55-273-6739
E-mail: atsushis@res.yamanashi-med.ac.jp

prolongation was compared between acute and chronic phase by administering proarrhythmic doses of non-specific I_{Kr} channel blocker cisapride (13, 18, 19). Finally, structural changes that may explain the electrophysiological adaptation were assessed using ECG gated MR images, in addition to photo- and electron-micrograph examinations.

MATERIALS AND METHODS

All experiments were carried out according to the Guidelines for Animal Experiments of Yamanashi Medical University, which are equivalent to those of the US National Institute of Health (NIH). Beagle dogs of either sex weighing about 10 kg were obtained through the Animal Laboratory for Research of Yamanashi Medical University.

Production of complete AV block

The dogs were anesthetized with pentobarbital sodium (30 mg/kg, i.v.) and artificially ventilated with room air (SN-480-3; Shinano, Tokyo). Tidal volume and respiratory rate were set at 20 ml/kg and 15 strokes/min, respectively. Heparin calcium (200 IU/kg, i.v.) was administered to prevent blood clotting. The surface lead II ECG and the systemic blood pressure at the right femoral artery were continuously monitored using a polygraph system (RM-6000; Nihon Kohden, Tokyo). A quadripolar electrodes catheter with a large tip of 4 mm (D7-DL-252; Cordis-Webster, Baldwin Park, CA, USA) was inserted through the right femoral vein using the standard percutaneous technique (20) under sterile condition and positioned passing the tricuspid valve watching the bipolar electrograms from the distal electrodes pair. The optimal site for the AV node ablation, namely the compact AV node, was determined on the basis of the intracardiac electrogram, of which a very small His deflection was recorded and atrium /ventricular voltage ratio was >2. The site was usually found at 1 – 2 cm proximal from the position where the largest His bundle electrogram was recorded. The power source for the AV node ablation was obtained from an electrosurgical generator (MS-1500; Mera, Tokyo) which delivers continuous unmodulated radiofrequency energy at a frequency of 500 kHz. After proper positioning, the radiofrequency energy of 20 W was delivered for 10 s from the tip electrode to an indifferent patch electrode positioned on the animal's back, which was followed by additional 30-s ablation if junctional rhythm was induced. The endpoint of this procedure was the development of the complete AV block with an onset of stable idioventricular escaped rhythm. Proper care was taken for the animals following the experimental period by the same experienced animal technician. The majority of the dogs were tested more than once. Five experimental protocols were carried out using these AV block animals at different time points after the induction of complete AV block.

Electrophysiological studies

Time course of the changes in the repolarization process of the AV block heart (Experiment 1): This study was repeated on the same animal group (n = 6) at 7 – 10 days (acute phase) and 28 – 56 days (chronic phase) after the induction of the complete AV block. The AV block dogs were anesthetized with pentobarbital sodium (30 mg/kg, i.v.). After intubation with a cuffed endotracheal tube, the animals were artificially ventilated with room air (SN-480-3, Shinano). Tidal volume and respiratory rate were set at 20 ml/kg and 15 strokes/min, respectively. The surface lead II ECG and the systemic blood pressure at the right femoral artery were continuously monitored using a polygraph system (RM-6000, Nihon Kohden). To prevent blood clotting, heparin calcium (100 IU/kg) was intravenously administered. A bi-directional steerable MAP recording/pacing combination catheter (1675P; EP Technologies Inc., Sunnyvale, CA, USA) was positioned at the endocardium of the interventricular septum of the right ventricle through the right femoral vein to obtain MAP signals. The signals were amplified with a DC pre-amplifier (300, EP Technologies, Inc.). The duration of the MAP signals was measured as an interval, along a line horizontal to the diastolic baseline, from the MAP upstroke to the desired repolarization level. The interval (ms) at 90% repolarization was defined as MAP_{90}, as previously reported (12 – 17).

The right ventricular septal wall was electrically driven using a cardiac stimulator (SEC-3102, Nihon Kohden) through the pacing electrodes of the combination catheter. The stimulation pulses were rectangular in shape, 1 – 2-V amplitude (about twice the threshold voltage) and 1-ms duration, which was kept during the experimental protocol. The MAP_{90} was measured at a pacing cycle length of 400, 500, 600, 750 or 1000 ms. The ERP was also assessed at the same site by the programmed electrical stimulation through the pacing electrodes of the combination catheter. The pacing protocol consisted of 8 beats of basal stimuli in a cycle length of 400, 500, 600, 750 or 1000 ms followed by an extra stimulus of various coupling intervals. Starting in the late diastole, the coupling interval was shortened in 5 – 10-ms decrement until refractoriness occurred. The post-repolarization refractoriness (PRR); namely $PRR = ERP - MAP_{90}$, was calculated at each basal pacing cycle length to estimate the extent of the electrical vulnerability of the heart, as previously described (12 – 17).

Time course of the susceptibility to a QT-prolonging drug (Experiment 2): Preponderance of arrhythmia was also examined in both the acute phase (n = 18) and chronic phase (n = 18) of the complete AV block. In each phase, ECG was assessed using a Holter recording and analyzing

system (Model 456A and Model 153; Del Mar Avionics, Irvine, CA, USA) as previously described (12, 21). About 2 h after the start of Holter ECG recording, the non-specific I_{Kr} blocker cisapride (19, 22, 23) in a dose of 1 mg/kg (low-dose group, n = 6) or 10 mg/kg (high-dose group, n = 6) was orally administered using a gelatin capsule to the animals without anesthesia. Meanwhile, a vacant capsule was administered to the control AV block animals (control group, n = 6). The drug doses used in this protocol were determined based on the previous reports (13, 18, 19, 22, 23). The ECG parameters at 1 h before the drug administration were defined as the control and the ECG was recorded for >20 h when lethal arrhythmia was not induced. In this study, TdP was defined as a polymorphic ventricular tachycardia associated with QT interval prolongation, consisting of five beats or more twisting QRS complexes around the baseline (4, 5, 8, 12, 23). Corrected QT interval (QTc) was obtained using the Bazett's formula (24).

Morphological studies

MR images (Experiment 3): This study was performed on the 1st, 45th and 90th day after the complete AV block to examine morphological changes of the heart with time (n = 4). The dogs were anesthetized with pentobarbital sodium (30 mg/kg, i.v.). After intubation with a cuffed endotracheal tube, the animals were transported to the MRI suite. T1-weighted images (TR/TE: 440/16) as well as ECG-gated MR images were obtained using a 0.2-T MR imager (Signa Profile, General Electric; Milwaukee, WI, USA). The short-axis view and 4-chamber view were used for assessment. The wall thickness and diameter of the left ventricle at end-diastole were measured on the short-axis view of the ECG-gated images.

Heart and body weights (Experiment 4): To assess the extent of hypertrophy after AV block, the heart and body weights of the sacrificed AV block animals in chronic phase (n = 13) were compared with those of control animals of normal sinus rhythm (n = 18). Additional data from another serious of experiments were also used.

Histology (Experiment 5): Histological studies were performed on the AV block hearts in chronic phase (n = 4) and the control hearts of normal sinus rhythm (n = 4). The animals were anesthetized with pentobarbital sodium (30 mg/kg, i.v.). After the hearts were removed and rinsed in saline, transmural specimens were obtained from the left ventricle, septal wall and right ventricle. These specimens were fixed in 10% neutrally buffered formaline and embedded in paraffin. Paraffin sections in 4-μm thickness were stained with hematoxylin-eosin (HE) and Azan and examined microscopically. Moreover, electron-microscopy was also performed to assess the changes. The formaline-fixed left ventricle was subjected to electron-microscopic examination. The tissue was minced into cubes, approximately 1-mm-thick, re-fixed in glutaraldehyde and osmium tetroxide, and embedded in Epon. Ultra-thin sections were stained with uranyl acetate and lead citrate and observed under a JEM 100CX transmission electron microscope (JEOL, Tokyo).

Drugs

Cisapride was extracted from a commercial source (Acenalin fine granules; Janssen-Kyowa, Tokyo), while heparin calcium (Mitsui, Tokyo) and pentobarbital sodium (Tokyo Kasei, Tokyo) were purchased.

Statistics

Data are presented as the mean ± S.E.M. Differences between groups were assessed using the unpaired *t*-test, one-way factorial ANOVA, Fisher's exact method for 2 × 2 cross table data or Chi square test, while those within a group were examined by either the paired *t*-test or one-way repeated-measures ANOVA followed by Contrasts for mean values comparison. *P*-value less than 0.05 was considered significant.

RESULTS

The AV node ablation successfully eliminated AV conduction in all animals (n = 30). The number of radiofrequency ablation trials was 1 – 2 in most of the cases. Stable idioventricular escaped rhythm always developed within 1 min after the onset of AV conduction block. This automaticity is considered to originate from the distal portion of AV junctional area, because of the relatively narrow QRS width with the right bundle branch block pattern. The mean blood pressure just after the AV block induction was within the physiological range of >80 mmHg in each animal. Two dogs died from the congestive heart failure during the 1st week of AV block, while in all other dogs, the complete AV block was maintained during the experimental period without any physical sign of decompensation.

Experiment 1: Changes in the MAP_{90}, ERP and PRR of the right ventricular septal wall

Six dogs were used for this analysis at the acute and chronic phases. Typical tracings of MAP at a pacing cycle length of 400 – 1000 ms in both acute and chronic phases from an animal are depicted in Fig. 1A, and the effects of basic pacing cycle length on the MAP_{90}, ERP and PRR are summarized in Fig. 1B. In the acute phase (n = 6), increasing the pacing cycle length from 400 to 1000 ms prolonged MAP_{90} from 202 ± 3 to 232 ± 6 ms and ERP from 213 ± 6 to 230 ± 6 ms, while PRR decreased from +10 ± 7 to –2 ± 9 ms. Also, in the chronic phase (n = 6), the MAP_{90} prolonged from 225 ± 12 to 284 ± 22 ms and ERP from

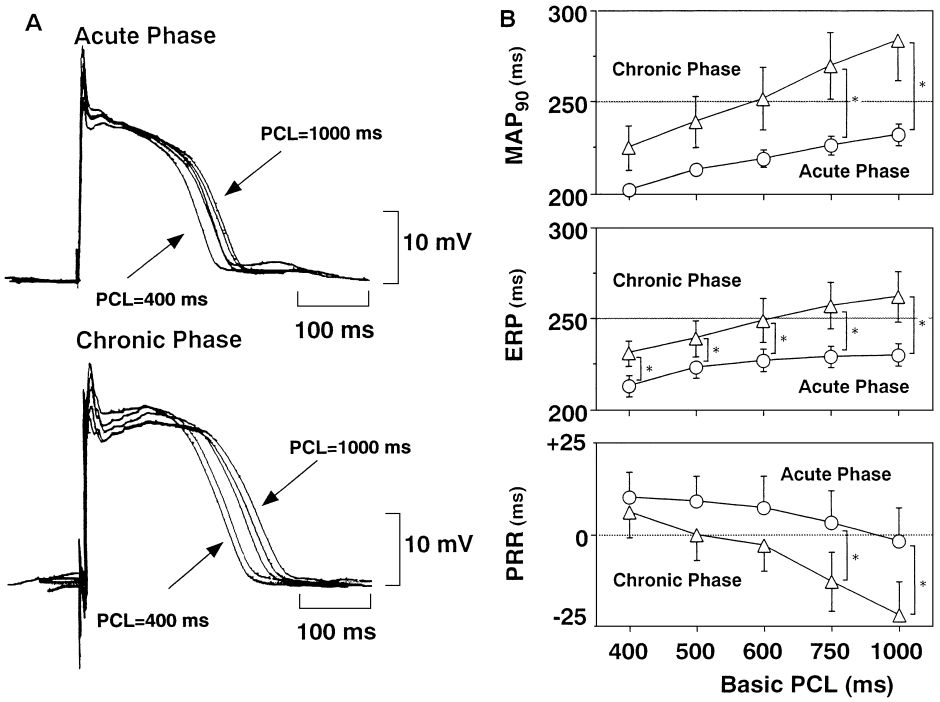

Fig. 1. Comparison of the effects of basic pacing cycle length (PCL) on the MAP_{90}, ERP and PRR between acute phase (7 – 10 days after the onset of AV block) and chronic phase animals (28 – 56 days after the onset of AV block). A: Typical tracings of MAPs. B: Summary of the results. Data are presented as the mean ± S.E.M. (n = 6). MAP_{90}: interval (ms) of the monophasic action potential at 90% repolarization level, ERP: effective refractory period, and PRR: post-repolarization refractoriness. **P*<0.05.

231 ± 7 to 262 ± 14 ms, while PRR changed from +6 ± 7 to –22 ± 9 ms. No early afterdepolarization was detected, but sporadic ventricular premature contractions were induced during the programmed electrical stimulation only in chronic phase. The MAP_{90} and ERP were longer and the PRR was more negative in the chronic phase as compared to those in the acute phase. Significant differences were detected between the acute and chronic phase animals in the MAP_{90} and PRR at the pacing cycle length of 750 and 1000 ms, while those were observed at each pacing cycle length in the ERP.

Experiment 2: Change in the response to proarrhythmic effects of cisapride

The proarrhythmic effects of cisapride are summarized in Fig. 2A, and typical tracings of ECG showing the cisapride-induced TdP are depicted in Fig. 2B. In the acute phase (n = 6 for each group), only sporadic ventricular premature contractions (PVCs) of <30 beats/h were induced in 3 animals out of 6 by low dose cisapride and 4 out of 6 by high dose cisapride. Meanwhile, no PVC was observed in the control group animals given vacant capsules. No TdP was induced in the acute phase.

In the chronic phase (n = 6 for each group), the number of animals that showed PVCs increased in both the low- and high-dose group. The number of PVCs was ≥30 beats /h in animals that showed TdP, while it was <30 beats/h in animals without TdP. TdP was induced in 1 animal out of 6 by low-dose cisapride and in all animals by high-dose cisapride. No TdP was observed in the control group. In one animal in the low-dose cisapride group and in 4 in the high-dose cisapride group, ventricular fibrillation finally occurred following TdP.

In animals that showed TdP, the duration of the non-fatal episode was 1 – 5 s and the rate of TdP was >300 beats/min (n = 5). TdP was preceded by a characteristic sequence of short/long/short cycles of R waves. No malignant ventricular arrhythmias were observed before the onset of TdP including sustained and/or monomorphic ventricular tachycardias. The first TdP appeared 7.6 ± 1.8 h after cisapride (n = 7). The elapsed time between the first TdP and the fatal TdP was 2.8 ± 1.4 h (0 – 6.0 h) (n = 5). The number of TdP recorded was 1 – 4 per each animal, and the last ventricular fibrillation was observed 9.4 ± 2.7 h after cisapride (n = 5).

Experiment 2: Change in the effects of cisapride on QTc

The time courses of ECG parameters and the number of surviving animals after cisapride are summarized in Fig. 3. In the acute phase (left panels), the idioventricular escaped rate (VR) (beats/min) and QTc (ms) at the pre-drug control

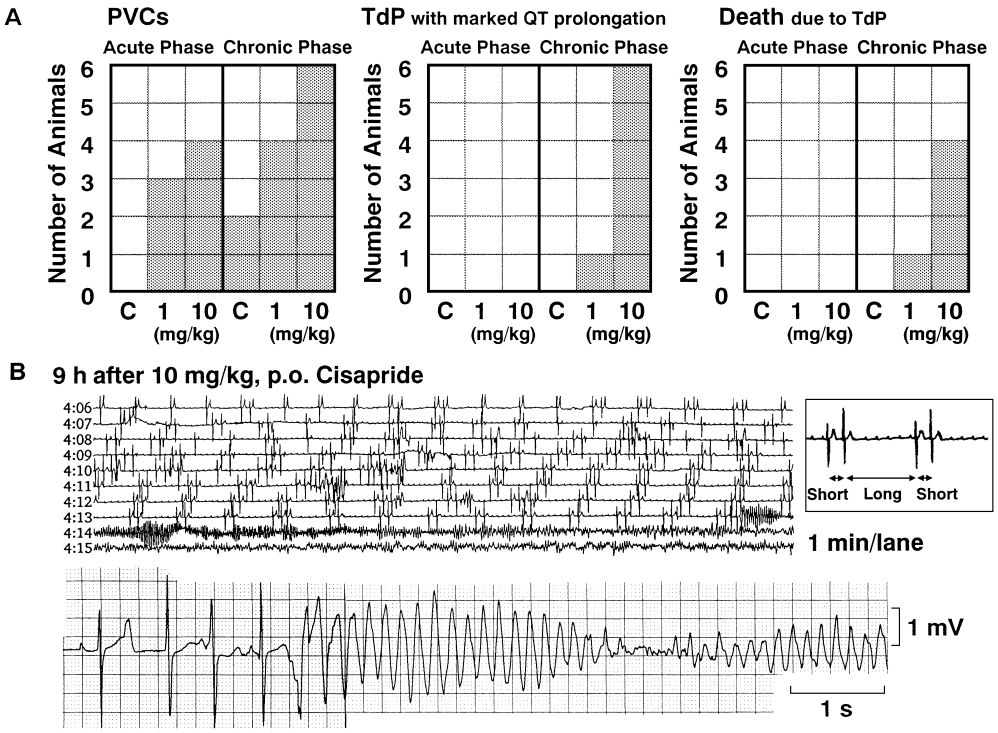

Fig. 2. Comparison of the susceptibility for torsade de pointes (TdP) between acute phase and chronic phase animals. A: Summary of the results. B: Compressed and continuous ECG image (lead II) of a dog complicating TdP. Note typical features of prolonged QT interval and short-long-short initiation sequence as shown in the rectangle. PVCs: premature ventricular contractions.

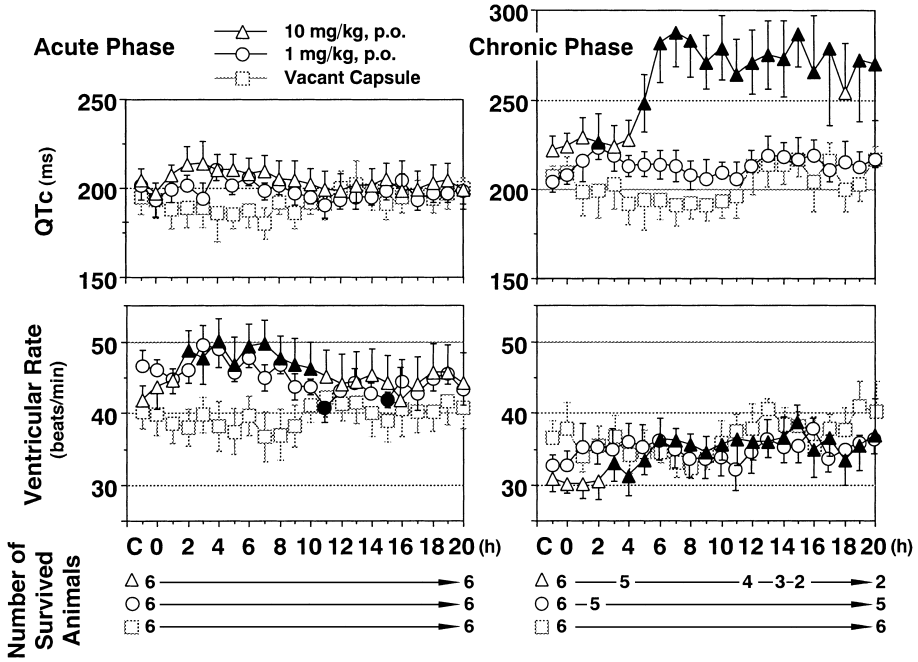

Fig. 3. Comparison of the effects of cisapride on QTc, ventricular rate and the number of surviving animals between acute phase and chronic phase animals. Closed symbols represent significant differences from each control value (C) at $P<0.05$. Data are presented as the mean ± S.E.M. Triangles: 10 mg of cisapride-administered group (n = 6), circles: 1 mg of cisapride-administered group (n = 6) and squares: vacant capsule-administered group (n = 6).

(C) were 40 ± 3 and 193 ± 10 in the control group (n = 6), 46 ± 2 and 193 ± 9 in the low dose cisapride group (n = 6) and 44 ± 3 and 197 ± 6 in the high dose cisapride group (n = 6), respectively. There were no differences in the pre-drug control values among the groups. After drug administration, VR decreased at 11 and 15 h in the low-dose cisapride group, but it increased for 2 – 10 h in the high-dose cisapride group, while no significant change was detected in the control group. No significant change was observed in QTc in any of these three groups, although there was a tendency of prolongation in the cisapride groups.

In the chronic phase (right panels), the VR (beats/min) and QTc (ms) at the pre-drug control (C) were 38 ± 4 and 209 ± 9 in the control group (n = 6), 33 ± 2 and 208 ± 5 in the low-dose-cisapride-administered group (n = 6), and 30 ± 1 and 224 ± 7 in the high-dose-cisapride-administered group (n = 6), respectively. There were no differences in the control values among the groups, but basal control QTc was longer and VR was slower in the chronic phase (n = 18) as compared to the acute phase (n = 18). After the drug administration, QTc was prolonged at 2 h, 5 – 17 h and 19 – 20 h in the high-dose-cisapride group, while no significant change was observed in the low-dose-cisapride group and control group, except that QTc was prolonged in one animal with complicating TdP by low dose cisapride. VR increased at 3 – 20 h in the high-dose-cisapride group, while no significant change was observed in the low-dose-cisapride and control groups.

Experiment 3: MR images

The time courses of the typical changes of the short-axis and 4 chamber views are depicted in Fig. 4, while those of the wall thickness and diameter of both ventricles are summarized in Table 1 (n = 4). The wall thickness and diameter of both ventricles increased during the initial 45 days after the induction of AV block. The hypertrophy

Table 1. Time course of the wall thickness and diameter of the ventricles

Days after onset of AVB			1st day	45th day	90th day
LV	Free wall	(mm)	6.2 ± 0.6	6.6 ± 0.4**	6.6 ± 0.4**
	Septal wall	(mm)	5.7 ± 0.2	7.2 ± 0.1**	7.2 ± 0.1**
	Diameter	(mm)	34.4 ± 0.4	45.9 ± 2.7**	48.3 ± 1.3**
RV	Free wall	(mm)	2.7 ± 0.1	3.4 ± 0.2*	4.0 ± 0.3**
	Diameter	(mm)	22.3 ± 1.7	26.8 ± 2.6**	27.8 ± 2.0**

AVB: atrioventricular block, LV: left ventricle, RV: right ventricle (mean ± S.E.M., n = 4). *P<0.05, **P<0.01 compared with the data on the 1st day.

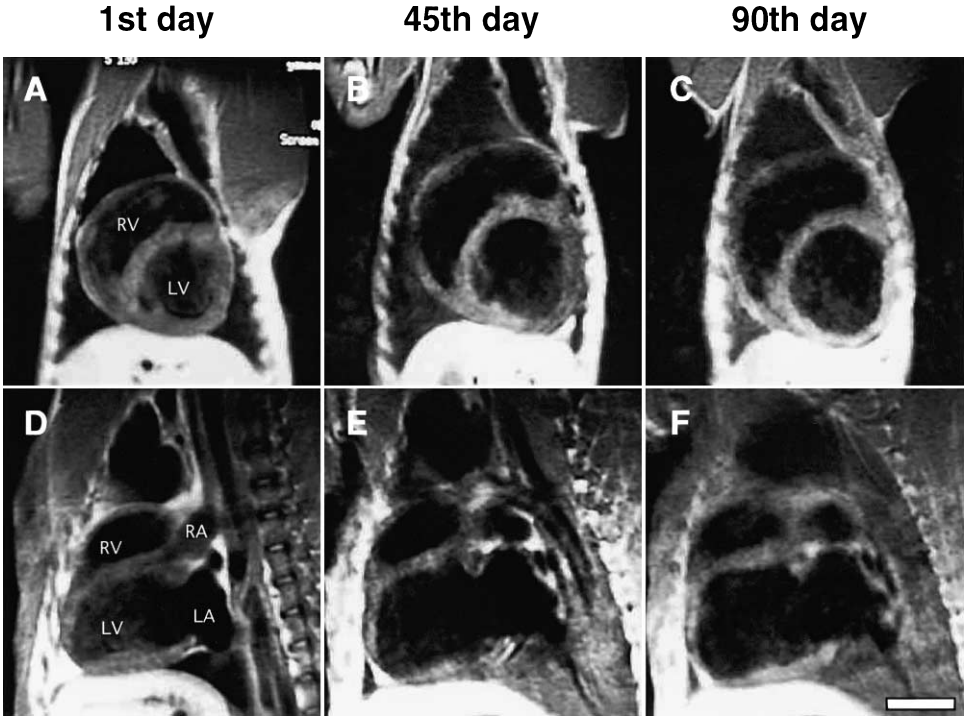

Fig. 4. The time courses of the changes of the short-axis (A, B and C) and 4 chamber views (D, E and F) in T1-weighted MR images. Temporal increase of both the ventricular size and slight increase of the wall thickness were demonstrated, thus showing an eccentric hypertrophy. Scale bar: 30 mm.

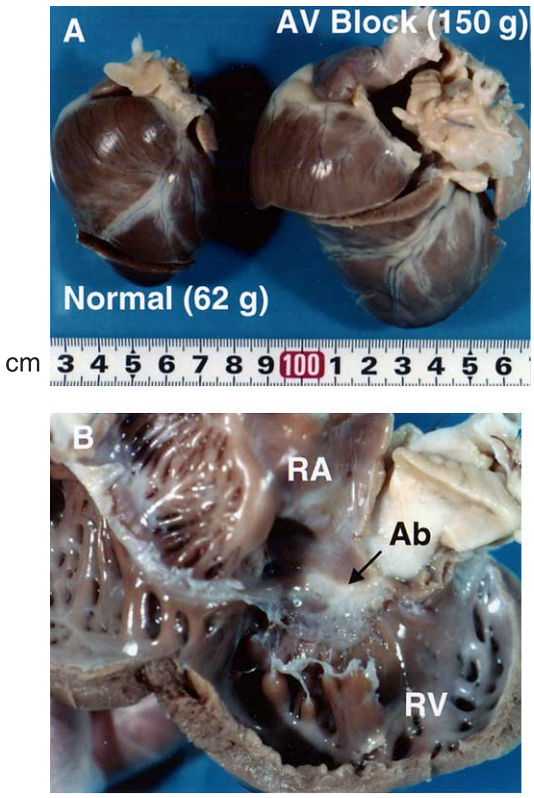

Fig. 5. Typical pictures of the AV block heart in the chronic phase. A: Comparison of a chronic AV block heart with a control heart of normal sinus rhythm. B: Right atrium (RA), AV nodal area and right ventricle (RV) of the AV block heart in the chronic phase. Note the white scar region in the AV nodal area where the radiofrequency energy would be applied (Ab).

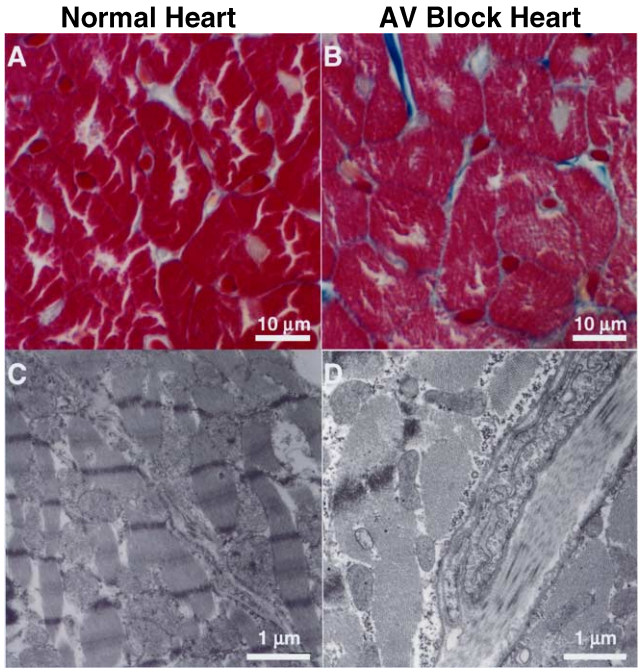

Fig. 7. Photo-micrographs (A and B: Azan stain) and electron-micrographs (C and D) of the left ventricular myocytes of the canine heart. A and C: Myocytes of the control heart of normal sinus rhythm. Few collagen fibers were seen in the intercellular space. B and D: Myocytes of the chronic AV block heart. The myocytes were markedly hypertrophied and collagen fiber was prominent compared with that of the control heart.

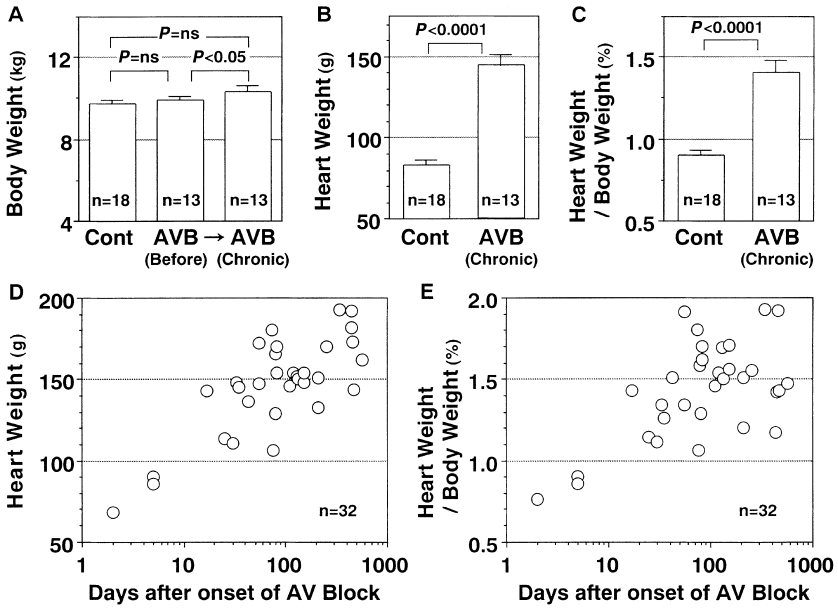

Fig. 6. Comparison of the body weight (A), heart weight (B) and heart/body weight (C) between control animals of normal sinus rhythm (Cont) or pre-operation animals (AVB Before) and chronic phase animals (AVB Chronic). The summary of the time courses of the heart weight (D) and heart/body weight (E) of the AV block animals. Data are presented as the mean ± S.E.M. AVB: atrioventricular block.

was eccentric. The degree of hypertrophy was greater in the right ventricular free wall (+25.9%) and septal wall (+26.3%) compared with that in the left ventricular free wall (+6.5%). On the other hand, no further change was observed during the 45th – 90th days.

Experiment 4: Changes in the body weight, heart weight and heart/body weight ratio

A typical AV block heart from a dog sacrificed in the chronic phase is depicted in Fig. 5 along with a normal control heart. The time courses of the heart weight and body weight of the AV block animals are summarized in Fig. 6. No significant difference was observed in the body weight between the control (n = 18) and the AV block animals (n = 13) both at the pre-operation period and 28 – 56 days after AV block. Meanwhile, the body weight of the AV block animals slightly increased from 9.9 ± 0.2 kg to 10.3 ± 0.3 kg during these 28 – 56 days after AV block (Fig. 6A). The heart weight and heart/body weight ratio were about 1.7 and 1.6 times greater in the AV block animals in the chronic phase as compared to the control animals, respectively (Fig. 6: B and C). The heart weight and heart/body weight ratio of the AV block animals increased to >100 g and >1% on 17th day after the onset of AV block, respectively (n = 32, Fig. 6: D and E).

Experiment 5: Histological changes

Typical photo-micrograph (A and B) and electron-micrograph (C and D) of the left ventricular myocytes of the normal control heart of sinus rhythm (A and C) and AV block heart in the chronic phase (B and D) are depicted in Fig. 7. Few collagen fibers were seen in the intercellular space in the normal control heart, while in the AV block heart, the collagen fibers and extracellular space increased, and each cardiomyocyte hypertrophied as compared to the normal control heart. These changes were confirmed in >90% fields from specimens of both ventricles assessed (n = 4).

DISCUSSION

The present electrophysiological and structural changes explain possible arrhythmogenic potential of the chronic AV block heart to QT-prolonging drugs developing to the degeneration of PVC to TdP. In the chronic AV block heart, both the "trigger" and "substrate" for the occurrence of TdP could increase, as will be discussed below.

Local proarrhythmic substrates

Previous studies (4, 5, 9) have suggested that interventricular dispersion of action potential duration predisposes the heart to the onset of TdP. The present electrophysiological analysis was designed to explore the local proarrhythmic substrates in the AV block heart. Right ventricular septal wall was assessed for this purpose, since less critical mass has been shown to be required to maintain ventricular fibrillation in the septal wall than in the right and left ventricular free walls (25). The final repolarization phase was analyzed by simultaneously measuring the ventricular MAP and ERP. Both ERP and MAP duration were prolonged in the chronic phase as compared with those of the acute phase, supporting the previous report that delayed rectifier potassium currents are down-regulated in the chronic AV block heart (6). More importantly, the prolongation of the MAP duration was more marked than that of the ERP in the chronic phase, particularly at a slower heart rate, indicating the prolongation of the electrically vulnerable period of the ventricle. These local electrophysiological changes indicate increase in the risk of aberrant excitation, which may provide a "substrate" for re-entry arrhythmias, leading to the onset of TdP (14, 15).

Induction of TdP by cisapride

There have been several reports describing that cisapride caused serious cardiac arrhythmias including TdP as a result of QT prolongation (18, 23). In vitro electrophysiological studies showed a possible mechanism of the proarrhythmic effects of cisapride to be its I_{Kr} blocking property (19, 23). In our previous study using the halothane-anesthetized canine in vivo models (13), intravenously administered at 1.0 mg/kg of cisapride prolonged the electrically vulnerable period in addition to prolonging ERP and MAP duration. Moreover, it induced a typical early afterdepolarization. The absolute bioavailability and elimination half-life ($T_{1/2}$) of oral cisapride are known to be about 40 – 50% and 7 – 10 h in healthy subjects, respectively (22). We administered 1 and 10 mg/kg, p.o. of cisapride to the AV block animals, although there may be potential species-related differences between man and dog in drug metabolism. Neither QTc prolongation nor lethal arrhythmia was initiated in the acute phase by either dose, while TdP following QTc prolongation was induced in one animal by the low dose and in all animals by the high dose in the chronic phase. More importantly, we provided evidence that short/long/short sequence is necessary for the onset of TdP, which has been referred to as the "cascade phenomenon" (10), suggesting that triggered activity due to early afterdepolarization might be occurring. Such premature impulse can be viewed as a "trigger" for re-entrant arrhythmias. Thus, cisapride-induced further prolongation of an already prolonged repolarization period in the chronic AV block heart may not only constitute the "substrate" for maintaining reentry to degenerate to TdP but also provide the "trigger".

Detection of drug-induced TdP

In a rabbit model for studying acquired long QT syndrome, infusion of cisapride in a dose of 3.0 μmol (= 1.452 mg) · kg^{-1} · 10 min^{-1} was associated with a significant lengthening of the QTU interval, but TdP appeared only in two rabbits out of six (23). In the present study, we demonstrated a higher incidence of TdP by p.o. administration of cisapride without anesthesia in the chronic AV block dogs. The higher sensitivity in this model can be explained by pre-drug existence of diminished potassium currents (4 – 6), resulting in the enhanced drug-induced QT prolongation. More importantly, this methodology has an important addition to the drug-induced TdP screening which till now was mostly performed under anesthesia using i.v. drug administration in the chronic AV block dog (4 – 10). Thus, our method in experiment 2 may become an alternative for detecting the torsadegenic action of drugs. Whether this method is suitable for predicting the occurrence of TdP in patients treated with such drugs has to be determined.

Anatomical adaptation

MR images indicated that significant eccentric hypertrophy of the chronic AV block heart. The degree of the hypertrophy was prominent in the right ventricular free wall and septal wall. These results are in good accordance with a recent report (26), indicating the reproducibility of the currently observed hypertrophic response after AV block induction. Moreover, the previous study (26) has demonstrated that the extent of each portion of the ventricular hypertrophy is closely associated with respective increases of AT1-receptor mRNA. Meanwhile, the heart weight of the chronic animals was 1.7 times greater than that of normal dogs with similar body weight, also confirming a previous publication (4). This type of anatomical remodeling of the heart may allow ventricular cavities to regain a normal wall stress (27), while these morphological changes may increase the risk of macroscopic re-entry in the chronic AV block heart, which could become the "substrate" of TdP. In addition, Fig. 6, D and E, may give the impression that the duration of AV block determines the heart weight, which is only the case in the beginning, but not after the adaptation point has been passed, which will be 2 – 4 weeks after the onset of AV block.

Histological adaptation

Photo- and electron-micrograph analyses showed myocardial cell hypertrophy together with the parallel increases of collagen fiber and extracellular space in the chronic phase. These findings are essentially in accordance with previous observations both in the canine chronic AV block heart (4) and in the right ventricular endomyocardial biopsy specimens from patients with documented AV block without apparent heart disease (28). These histological changes might indicate a physiological adaptation of the contractile muscle and connective tissue network to maintain normal ventricular function (4), which may be the reason for the lack of congestive heart failure in chronic phase animals. However, the myocardial cell hypertrophy may increase action potential duration (5) and the increases of collagen fiber and extracellular space will uncouple the constituent cardiac myocytes (29). Thus, these structural changes can be the "substrate" that may explain the enhanced susceptibility of the chronic stage heart to QT-prolonging drugs and occurrence of TdP.

Conclusions

While electrical and structural changes in the chronic AV block heart might be aimed to maintain cardiac function, they also predispose the heart to the drug-induced QT prolongation with enhanced risk of re-entry and early afterdepolarization, leading to the onset of TdP. Thus, the present canine model of TdP can be used to screen new agents with QT prolonging effects for their proarrhythmic potentials. These results also suggest that patients with ventricular hypertrophy and persistent bradycardia may be more susceptible to proarrhythmic effects of QT-prolonging agents.

Acknowledgments

The authors thank Dr. H. Shiina and Mr. S. Shimizu for their skillful technical assistance.

REFERENCES

1 Tamargo J: Drug-induced torsade de pointes: from molecular biology to bedside. Jpn J Pharmacol **83**, 1 – 19 (2000)

2 Eckardt L, Haverkamp W, Borggrefe M and Breithardt G: Experimental models of torsade de pointes. Cardiovasc Res **39**, 178 – 193 (1998)

3 Weissenburger J, Chezalviel F, Davy JM, Lainee P, Guhennec C, Penin E, Engel F, Cynober L, Motte G and Cheymol G: Methods and limitation of an experimental model of long QT syndrome. J Pharmacol Methods **26**, 23 – 42 (1991)

4 Vos MA, de Groot SHM, Verduyn SC, van der Zande J, Leunissen HDM, Cleutjens JPM, van Bilsen M, DaemenMJAP, Schreuder JJ, Allessie MA and Wellens HJJ: Enhanced susceptibility for acquired torsade de pointes arrhythmias in the dog with chronic, complete AV block is related to cardiac hypertrophy and electrical remodeling. Circulation **98**, 1125 – 1135 (1998)

5 Volders PGA, Sipido KR, Vos MA, Kulcsár A, Verduyn SC and Wellens HJJ: Cellular basis of biventricular hypertrophy and arrhythmogenesis in dogs with chronic complete atrioventricular block and acquired torsade de pointes. Circulation **98**, 1136 – 1147 (1998)

6 Volders PGA, Sipido KR, Vos MA, Spätjens RLHMG and Leunissen JDM: Downregulation of delayed rectifier K^+ currents in dogs with chronic complete atrioventricular block and acquired torsades de pointes. Circulation **100**, 2455 – 2461 (1999)

7 de Groot SHM, Schoenmakers M, Molenschot MMC, Leunissen JDM, Wellens HJJ and Vos MA: Contractile adaptations preserving cardiac output predispose the hypertrophied canine heart to delayed afterdepolarization-dependent ventricular arrhythmias. Circulation **102**, 2145 – 2151 (2000)
8 Vos MA, Verduyn SC, Gorgels APM, Lipcsei GC and Wellens HJJ: Reproducible induction of early afterdepolarizations and torsade de pointes arrhythmias by *d*-sotalol and pacing in dogs with chronic atrioventricular block. Circulation **91**, 864 – 872 (1995)
9 Verduyn SC, Vos MA, van der Zande J, van der Hulst FF and Wellence HJJ: Role of interventricular dispersion of repolarization in acquired torsade-de-pointes arrhythmias: reversal by magnesium. Cardiovasc Res **34**, 453 – 463 (1997)
10 Vos MA, Gorenek B, Verduyn SC, van der Hulst FF and Leunissen JD: Observations on the onset of Torsade de Pointes arrhythmias in the acquired long QT syndrome. Cardiovasc Res **48**, 421 – 429 (2000)
11 El-Sherif N, Caref EB, Yin H and Restivo M: The electrophysiological mechanism of ventricular arrhythmias in the long-QT syndrome: tridimensional mapping of activation and recovery patterns. Circ Res **79**, 474 – 492 (1996)
12 Chiba K, Sugiyama A, Satoh Y, Shiina H and Hashimoto K: Proarrhythmic effects of fluoroquinolone antibacterial agents: In vivo effects as physiologic substrate for Torsades. Toxicol Appl Pharmacol **169**, 8 – 16 (2000)
13 Sugiyama A and Hashimoto K: Effects of gastrointestinal prokinetic agents, TKS159 and cisapride, on the in situ canine heart assessed by cardiohemodynamic and electrophysiological monitoring. Toxicol Appl Pharmacol **152**, 261 – 269 (1998)
14 Franz MR and Costard A: Frequency-dependent effects of quinidine on the relationship between action potential duration and refractoriness in the canine heart in situ. Circulation **77**, 1177 – 1184 (1988)
15 Kirchhof PF, Fabritz CL and Franz MR: Postrepolarization refractoriness versus conduction slowing caused by class I antiarrhythmic drugs: Antiarrhythmic and proarrhythmic effects. Circulation **97**, 2567 – 2574 (1998)
16 Satoh Y, Sugiyama A, Tamura K and Hashimoto K: Effects of a class III antiarrhythmic drug, dofetilide, on the in situ canine heart assessed by the simultaneous monitoring of hemodynamic and electrophysiological parameters. Jpn J Pharmacol **81**, 79 – 85 (1999)
17 Sugiyama A, Aye NN, Katahira S, Saitoh M, Hagihara A, Matsubara Y and Hashimoto K: Effects of nonsedating antihistamine, astemizole, on the in situ canine heart assessed by cardiohemodynamic and monophasic action potential monitoring. Toxicol Appl Pharmacol **143**, 89 – 95 (1997)
18 Ahmad SR and Wolfe SM: Cisapride and torsades de pointes. Lancet **345**, 508 (1995)
19 Drolet B, Khalifa M, Daleau P, Hamelin BA and Turgeon J: Block of the rapid component of the delayed rectifier potassium current by the prokinetic agent cisapride underlies drug-related lengthening of the QT interval. Circulation **97**, 204 – 210 (1998)
20 Baim DS and Grossman W: Percutaneous approach including trans-septal and apical puncture. *In* Cardiac Catheterization, Angiography, and Intervention, 5th ed, Edited by Baim DS, pp 57 – 81, Williams & Wilkins, Baltimore (1995)
21 Akie Y, Ni C, Aye NN, Xue YX and Hashimoto K: Proarrhythmic effects of four class III antiarrhythmic drugs, MS-551, sematilide, dofetilide and KCB328, examined using ambulatory ECG. Asia Pacific J Pharmacol **14**, 101 – 109 (2000)
22 Wiseman LR and Faulds D: Cisapride. Drugs **47**, 116 – 152 (1994)
23 Carlsson L, Amos GJ, Andersson AB, Drews L, Duker G and Wadstedt G: Electrophysiological characterization of the prokinetic agents cisapride and mosapride in vivo and in vitro: Implications for proarrhythmic potential? J Pharmacol Exp Ther **282**, 220 – 227 (1997)
24 Bazett HC: An analysis of the time-relations of electrocardiogram. Heart **7**, 353 – 370 (1920)
25 Ikeda T, Kawase A, Nakazawa K, Ashihara TT, Namba TT, Takahashi TK, Sugi K and Yamaguchi T: Role of structural complexities of septal tissue in maintaining ventricular fibrillation in isolated, perfused canine ventricle. J Cardiovasc Electrophysiol **12**, 66 – 75 (2001)
26 Verduyn SC, Ramakers C, Snoep G, Leunissen JDM, Wellens HJJ and Vos MA: Time course of structural adaptations in chronic AV block dogs: evidence for differencial ventricular remodeling. Am J Physiol **280**, H2882 – H2890 (2001)
27 Opie LH: The Heart, Physiology, From Cell to Circulation, 3rd ed, Lippincott-Raven Publishers, Philadelphia (1998)
28 Teragaki M, Toda I, Sakamoto K, Shimada K, Yamagishi H, Yoshiyama M, Akioka K, Kawase Y, Nishimoto M, Takeuchi K and Yoshikawa J: Endomyocardial biopsy findings in patients with atrioventricular block in the absence of apparent heart disease. Heart Vessels **14**, 170 – 176 (1999)
29 Peters NS and Wit AL: Myocardial architecture and ventricular arrhythmogenesis. Circulation **97**, 1746 – 1754 (1998)